BOREAL ENVIRONMENT RESEARCH 24: 201–214
ISSN 1797-2469 (online)

Helsinki 11 November 2019

Observed annual surface ozone maxima and minima in northern and central Europe from 1990–2015 — latitude dependence and temporal trends

Jenny Klingberg[1)2)*], Per Erik Karlsson[3)], Camilla Andersson[4)], Magnuz Engardt[4)5)†], Gunilla Pihl Karlsson[3)] and Håkan Pleijel[2)]

[1)] *Gothenburg Botanical Garden, Carl Skottsbergs Gata 22A, SE-41319 Göteborg, Sweden (*corresponding author's e-mail: jenny.klingberg@vgregion.se)*
[2)] *University of Gothenburg, Biological and Environmental Sciences, P.O. Box 461, SE-40530 Göteborg, Sweden*
[3)] *IVL Swedish Environmental Research Institute Inc., P.O. Box 53021, SE-40014 Göteborg, Sweden*
[4)] *Swedish Meteorological and Hydrological Institute, SE-60176 Norrköping, Sweden*
[5)] *Environmental and Health Administration, Box 8136, SE-104 20 Stockholm, Sweden*
[†] *Present address*

Received 02 Jul. 2019, final version received 02 Oct. 2019, accepted 02 Oct. 2019

Klingberg J., Karlsson P., Andersson C., Engardt M., Pihl Karlsson G. & Pleijel H. 2019: Observed annual surface ozone maxima and minima in northern and central Europe from 1990–2015 — latitude dependence and temporal trends. *Boreal Env. Res.* 24: 201–214.

Ground-level ozone is an air pollutant that, despite reductions in precursor emission in Europe, still represents a risk to vegetation and human health. This study is based on observations of ozone concentrations ($[O_3]$) from 25 European monitoring stations, north of the Alps within the EMEP network, during the 26-year period from 1990–2015. We analyzed the maximum and minimum hourly $[O_3]$ as well as the seasonal cycle in relation to latitude. In addition, temporal trends were studied. The maximum $[O_3]$ increased towards the south of the study area, while the yearly minimum of daytime mean increased towards the north. There was a strong correlation between the day of year when the maximum $[O_3]$ occurred and latitude: the maximum $[O_3]$ occurred earlier in the north. The maximum daytime $[O_3]$ decreased at all stations while the minimum daytime $[O_3]$ increased at most stations during the studied time period.

Introduction

Tropospheric ozone (O_3) is a photochemical pollutant produced from the precursors nitrogen oxides ($NO_x = NO + NO_2$), volatile organic compounds (VOCs) including methane (CH_4) and carbon monoxide (CO), under the influence of solar radiation. O_3 is involved in a large number of environmental problems, which include adverse health effects (WHO 2006), damage to crops and forests (Royal Society 2008) and is an important greenhouse gas (IPCC 2013).

Observations and modelling studies point toward a decrease in high ozone concentration ($[O_3]$) levels in large parts of Europe due to reductions in European emissions of O_3 precursors (Solberg *et al*. 2005, Paoletti *et al*. 2014, Sicard *et al*. 2016, Karlsson *et al*. 2017). At the same time there is strong evidence that hemi-

Editor in charge of this article: Veli-Matti Kerminen

spheric background [O_3] have been increasing until recently (Parrish *et al*. 2012, Monks *et al*. 2015). In Europe, [O_3] levels are changing and European emission changes alone cannot explain the changes in [O_3] that are observed (Jonson *et al*. 2006, Andersson *et al*. 2017).

Measurements of [O_3] throughout the troposphere clearly show an annual variation, which at certain locations exhibit a distinct maximum during spring. The spring O_3 maximum is a Northern Hemispheric phenomenon, where it occurs widely across the mid-latitudes (Monks 2000, Vingarzan 2004). There are also latitude/longitude gradients in the shape of the seasonal cycle over Europe. Polluted continental sites are characterized by a broad summer maximum whereas clean unpolluted sites have a spring [O_3] maximum (Jonson *et al*. 2006).

A distinct spring maximum and late summer minimum in surface [O_3] has been observed at sites in northern Sweden (> 64°N) (Klingberg *et al*. 2009) as well as at other sites in the European Arctic (Rummukainen *et al*. 1996, Narayana Rao *et al*. 2004). Also, in the western parts of Europe, there are sites with a spring [O_3] maximum and summer minimum, e.g., Mace Head on the North Atlantic Ocean coastline of Ireland (Derwent *et al*. 2018); while in the interior of Europe, measurements show a broad summer maximum (Monks 2000). The results of an O_3 reanalysis for Sweden by Andersson *et al*. (2017) show a higher spring maximum in the north compared with the south and a shift of the maximum to earlier in the year.

The seasonal cycle of [O_3] in the troposphere is controlled by several processes acting on different spatial and temporal scales. The two main processes contributing to the spring [O_3] maximum are thought to be a stratospheric–tropospheric exchange and photochemical production in the troposphere (Monks 2000). There is an ongoing discussion about the relative importance of these processes (Monks 2000, Kim and Lee 2010).

The spring O_3 dynamics may be regarded as a proxy for the changes in atmospheric composition due to human activities (Monks 2000). A better understanding of the spring [O_3] maximum, the mechanisms that lead to its formation and its geographical pattern is important in the context of contemporary and future risk assessment for O_3 effects on both human health and vegetation.

For the safety of human health, the environmental quality standards (EQS) indicate that as a long-term objective, the daily maximum running 8-hour mean near-surface [O_3] must not exceed 120 μg m^{-3} (EU 2008) or even 100 μg m^{-3} (WHO 2006). [O_3] are generally considerably lower over northern Europe compared with continental and southern Europe. However, an increasing trend in the spring [O_3] maximum, as found in e.g., northern Sweden (Karlsson *et al*. 2007), may decrease the possibility to reach the EQS in this region.

The EQS metric used within the EU legislation for the protection of vegetation is the accumulated exposure over the threshold of 40 ppb (AOT40) during the three-month period from May–July (EU 2008). The target value is not to exceed 9000 ppb hours averaged over five years. The long-term objective is a May–July AOT40 below 3000 ppb hours.

Presently, the growing season largely starts after the O_3 spring maximum in northernmost Europe (Karlsen *et al*. 2008), but a number of studies have shown an earlier onset of spring and a lengthening of the growing season in middle and high latitudes, likely associated with global warming (Linderholm 2006, Menzel *et al*. 2006, Karlsson *et al*. 2007). An increasing overlap between the spring [O_3] maximum and the growing season could lead to an increased risk of O_3 effects on vegetation in this region, if the current seasonal O_3 cycle persists (Karlsson *et al*. 2007, Klingberg *et al*. 2009).

It is thus of large importance to consolidate our understanding of geographical patterns as well as trends in level and timing of annual [O_3] maximum. It will have implications both for the possibility to meet the O_3 EQS for human health, vegetation and for the development of efficient abatement strategies.

The aim of this investigation was to assess the level and timing of the annual maximum in [O_3] in relation to latitude for the 26-year period of 1990–2015 in Europe north of the Alps. Further, changes in the timing of the annual [O_3] maximum was studied since this may affect the

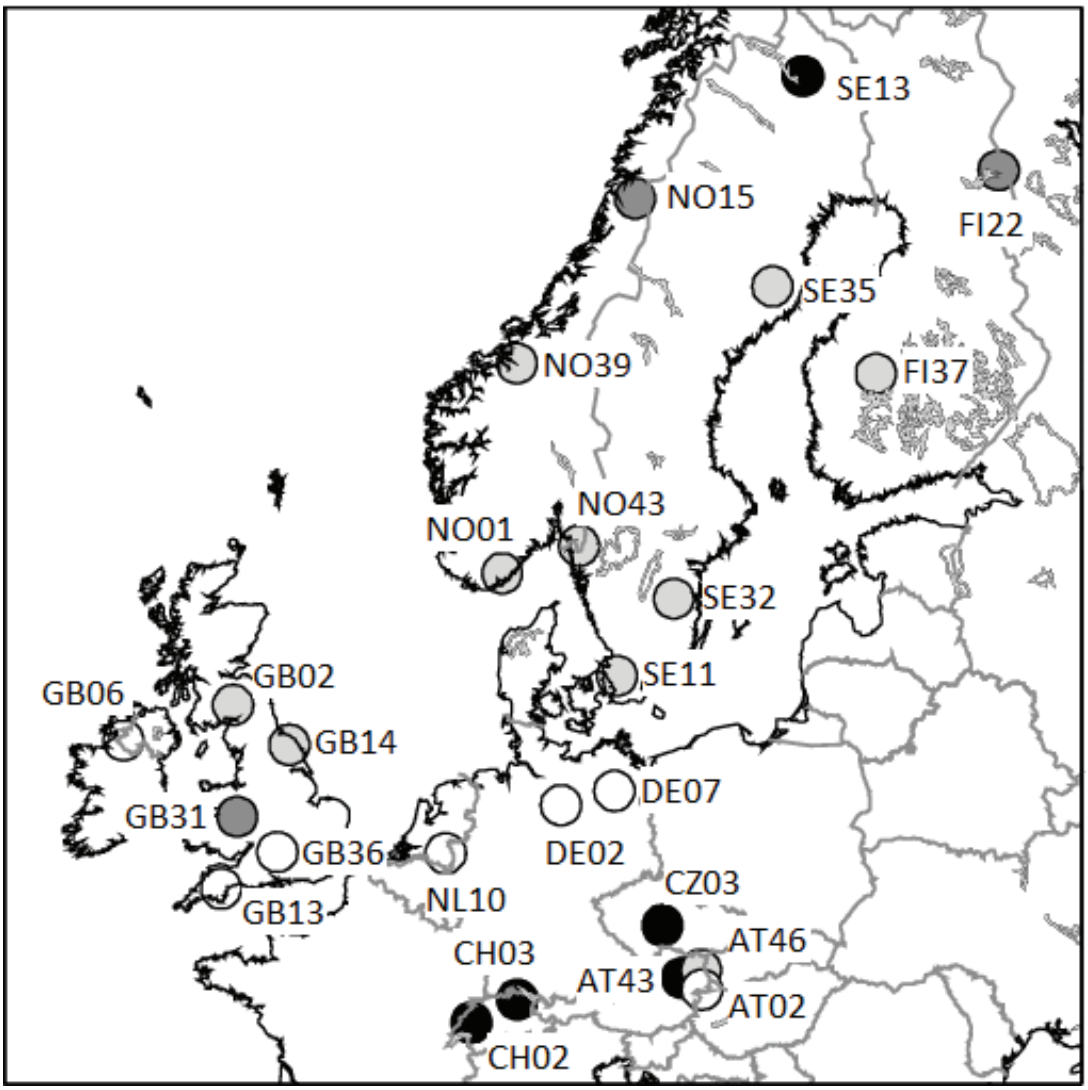

Fig. 1. Map of locations of the 25 EMEP monitoring sites included in the study. Station ID are shown according to Table 1. Colored circles indicate altitude of the stations above sea level, white 0–150 m, light grey 150–300 m, dark grey 300–450 m and black 450–600 m.

risk assessment of O_3. The temporal development of the lower fractions of $[O_3]$ was also investigated to detect potential changes in the general (hemispheric) background $[O_3]$. Our hypotheses were: 1) the annual maximum in $[O_3]$ occurs earlier at higher latitude; 2) the spring/summer maximum in $[O_3]$ represents a larger fraction of the annual O_3 exposure at higher latitudes; and the $[O_3]$ maxima are decreasing over time while $[O_3]$ in the lower range of concentrations are increasing.

Data and methods

To study the yearly dynamics of the surface $[O_3]$, 25 monitoring stations within the European Monitoring and Evaluation Programme, EMEP were selected covering the period 1990–2015. Hourly $[O_3]$ were obtained from the EMEP database (available at http://ebas.nilu.no; see Torseth *et al*. (2012)). The selection criteria used were: 1) long time series, i.e., at least 20 years with less than 10% data missing per year

since 1990; 2) the altitude of the stations must be less than 600 m above sea level since mountain areas have been observed to experience higher [O_3] than the adjacent lowland (Klingberg *et al*. 2009); and 3) the station should not be located directly along the coast or close to large water surface since a marine influence can effect [O_3] strongly (Pleijel *et al*. 2013).

A maximum of two stations per latitude band were selected, the ones with the least data coverage was excluded. The study area was confined to Europe, north of the Alps. The location of the stations ranged from Austria and Switzerland to the south, Northern Ireland to the west and to the Arctic Circle in Sweden and Finland. Note that data from Mace Head is excluded from our analysis due to the station's failure to meet the third criteria above. More information about the monitoring stations included in the study can be found in Fig. 1 and Table 1.

For data loss up to 5 consecutive hours, the missing data were replaced by linear interpolation. In the case of 6–24 consecutive hours missing, the data were replaced by an average of the values for the same hour of the day before and the day after. Daytime [O_3] was used throughout the study to avoid the potentially very strong effect on [O_3] near the ground following nocturnal inversions; the strength of which is defined by local meteorology (Klingberg *et al*. 2012). Daytime was defined as the 12-hour period from 08:00–20:00 local time.

The accumulated exposure over the threshold of X ppb (AOTX_P) was calculated during daytime (08:00–20:00 local time) as described by Fuhrer *et al*. (1997):

$$\mathrm{AOT}X_P = \sum \max \Delta t\,([\mathrm{O_3}] - X, 0), \qquad (1)$$

where X is the [O_3] threshold in ppb, [O_3] is the hourly [O_3], Δt is the time step (1 hour) and P denotes the period over which the sum-

Table 1. ID, name, coordinates, altitude (m a.s.l.), the number of years (*N*) with less than 10% of data missing between 1990 and 2015 for the 25 EMEP monitoring stations included in the study and the time zone of the station.

ID	Name	Latitude	Longitude	Altitude (m)	Years with data (*N*)	Time zone
SE13	Esrange	67°53′00′′N	21°04′00′′E	475	1991–2015 (24)	UTC+1
FI22	Oulanka	66°19′13′′N	29°24′06′′E	310	1990–2015 (23)	UTC+2
NO15	Tustervatn	65°50′00′′N	13°55′00′′E	439	1990–2015 (25)	UTC+1
SE35	Vindeln	64°15′00′′N	19°46′00′′E	225	1990–2015 (25)	UTC+1
NO39	Kårvatn	62°47′00′′N	08°53′00′′E	210	1992–2015 (24)	UTC+1
FI37	Ähtäri (1 &) 2	62°35′00′′N	24°11′00′′E	180	1990–2015 (23)	UTC+2
NO43	Prestebakke	59°00′00′′N	11°32′00′′E	160	1990–2015 (24)	UTC+1
NO01	Birkenes (1 &) 2	58°23′18′′N	08°15′07′′E	219	1990–2015 (20)	UTC+1
SE32	Norra Kvill	57°49′00′′N	15°34′00′′E	261	1990–2015 (26)	UTC+1
SE11	Vavihill	56°01′00′′N	13°09′00′′E	175	1990–2015 (26)	UTC+1
GB02	Eskdalemuir	55°18′47′′N	03°12′15′′W	243	1990–2015 (25)	UTC
GB06	Lough Navar	54°26′35′′N	07°52′12′′W	126	1990–2015 (21)	UTC
GB14	High Muffles	54°20′04′′N	00°48′27′′W	267	1990–2015 (20)	UTC
DE07	Neuglobsow	53°10′00′′N	13°02′00′′E	62	1992–2015 (23)	UTC+1
DE02	Waldhof	52°48′08′′N	10°45′34′′E	74	1990–2015 (24)	UTC+1
GB31	Aston Hill	52°30′14′′N	03°01′59′′W	370	1990–2015 (20)	UTC
GB36	Harwell	51°34′23′′N	01°19′00′′W	137	1990–2015 (23)	UTC
NL10	Vredepeel	51°32′28′′N	05°51′13′′E	28	1990–2015 (24)	UTC+1
GB13	Yarner Wood	50°35′47′′N	03°42′47′′W	119	1990–2015 (20)	UTC
CZ03	Kosetice (NOAK)	49°35′00′′N	15°05′00′′E	534	1994–2015 (21)	UTC+1
AT46	Gänserndorf	48°20′05′′N	16°43′50′′E	161	1991–2015 (24)	UTC+1
AT43	Forsthof	48°06′22′′N	15°55′10′′E	581	1990–2015 (24)	UTC+1
AT02	Illmitz	47°46′00′′N	16°46′00′′E	117	1990–2015 (26)	UTC+1
CH03	Tänikon	47°28′47′′N	08°54′17′′E	539	1991–2015 (25)	UTC+1
CH02	Payerne	46°48′47′′N	06°56′41′′E	489	1991–2015 (25)	UTC+1

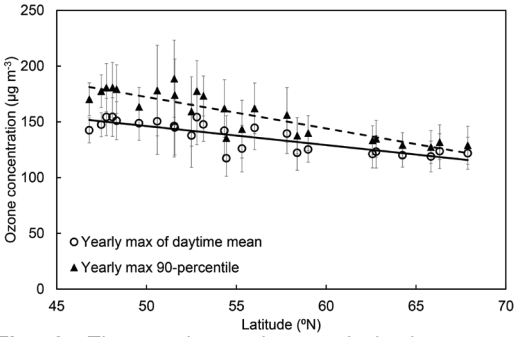

Fig. 2. The yearly maximum of daytime mean (08:00–20:00 local time) and yearly maximum of the daily 90th percentile in ozone concentration, as an average from the years 1990–2015, in relation to the latitude of the monitoring station. Error bars show ±1 SD. Yearly maximum of daytime mean: $y = -1.7x + 231.4$, $R^2 = 0.69$, $p < 0.001$. Yearly maximum of the 90th percentile: $y = -2.8x + 313.2$, $R^2 = 0.78$, $p < 0.001$.

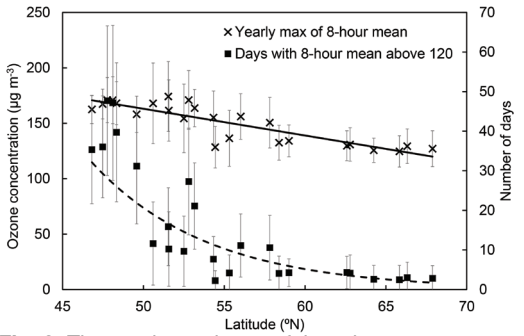

Fig. 3. The yearly maximum of the 8-hour mean ozone concentration (left axis) as well as the number of days the 8-hour mean exceeded 120 μg m^{-3} (right axis), as an average from the years 1990–2015, in relation to the latitude of the monitoring station. Error bars show ±1 SD. Yearly maximum of 8-hour mean: $y = -2.4x + 283.8$, $R^2 = 0.76$, $p < 0.001$. Days with 8-hour mean above 120: $y = 21400e-0.14x$, $R^2 = 0.74$, $p < 0.001$.

mation is performed, May–July or peak (see section: Accumulated O_3 exposure). The May–July AOT40 is used as the environmental quality standard (EQS) for the protection of vegetation within the EU legislation. However, the AOT index has a larger sensitivity to [O_3] at higher threshold values, as demonstrated by Tuovinen (2000) and Tuovinen *et al*. (2007). In this study, AOT was therefore calculated without using a threshold (AOT0), the threshold 30 ppb (AOT30) and the threshold 60 ppb (AOT60) in addition to AOT40. Only years with less than 10% data missing during the period over which AOT*X* was accumulated was used in the analysis.

Latitudinal variations of different O_3 indices were studied by fitting linear or exponential models of the average station data against latitude through regression analysis. Pearson Product-moment Correlation Coefficient was used to estimate the strength of the relationship and the statistical significance of the correlation was estimated using Student's *t*-test. The statistical significance of trends in time was analyzed using the Mann-Kendall trend test (Mann 1945) and Sen's slope (Sen 1968). Mann-Kendall is a non-parametric test widely used to detect increasing or decreasing trends in time series of data. The method is not sensitive to outliers or missing values.

Results

Annual [O_3] maximum and minimum in relation to latitude

The yearly [O_3] dynamics differed considerably within the study area. However, when data was aggregated over many years and stations, clear patterns appeared. The yearly maximum, as an average from 1990–2015, declined with increasing latitude (Fig. 2). This was independent of whether the index yearly maximum of the daytime mean [O_3] or yearly maximum of the 90th percentile of [O_3] was used. The relationships were strongly significant ($p < 0.001$). There were strong and statistically significant ($p < 0.001$) negative correlations between the daily maximum 8-hour mean [O_3] and latitude, and between the number of days with the maximum 8-hour mean [O_3] > 120 µg m^{-3} and latitude (Fig. 3). The latitude of the monitoring stations did not correlate with the altitude. Consequently, the altitude was not a confounding factor (data not shown). The yearly minimum of the daytime mean [O_3] was higher towards the north (Fig. 4).

The average day of the year when the yearly maximum [O_3] occurred, as an average from 1990–2015, declined strongly and significantly with an increasing latitude (Fig. 5). This means that the annual maximum in [O_3] has been shifted

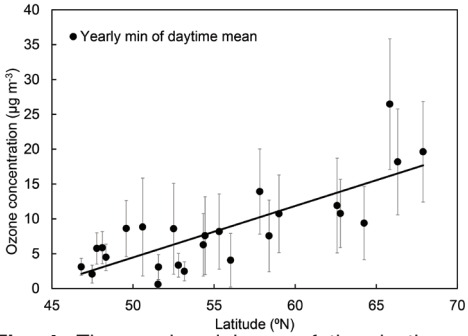

Fig. 4. The yearly minimum of the daytime mean (08:00–20:00 local time) in ozone concentration, as an average from the years 1990–2015, in relation to the latitude of the monitoring station. Error bars show ±1 SD. Yearly minimum of the daytime mean: $y = 0.74x - 32.5$, $R^2 = 0.63$, $p < 0.001$.

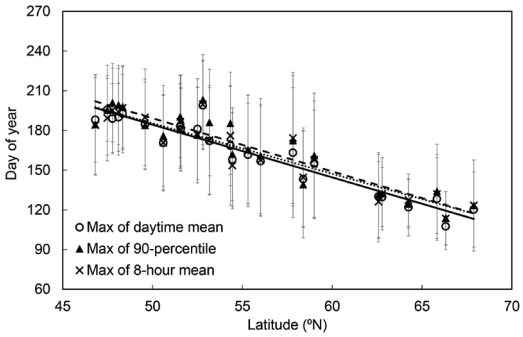

Fig. 5. Day of year when the yearly maximum of the daytime mean, the maximum of daily 90th percentile and the maximum 8-hour mean occurred, as an average from the years 1990–2015, in relation to the latitude of the monitoring station. Error bars show ±1 SD. The maximum of the daytime mean: $y = -4.0x + 383.5$, $R^2 = 0.91$, $p < 0.001$. The maximum of the of 90th percentile: $y = -4.0x + 390.3$, $R^2 = 0.87$, $p < 0.001$. The maximum 8-hour mean: $y = -3.8x + 376.6$, $R^2 = 0.87$, $p < 0.001$.

from the summer in the southern part of the region to spring in the north. The day of the year when $[O_3]$ maximum occurred was not sensitive to the choice of indicator for $[O_3]$ maximum, since all three metrics of the maximum $[O_3]$ showed essentially the same relationship with latitude. The small variation between monitoring stations (Fig. 5) indicates that the longitude of the station did not substantially affect the day of year of maximum $[O_3]$. Tests showed that the influence of occasional episodes of high $[O_3]$ on the day of year of maximum $[O_3]$ in Fig. 5

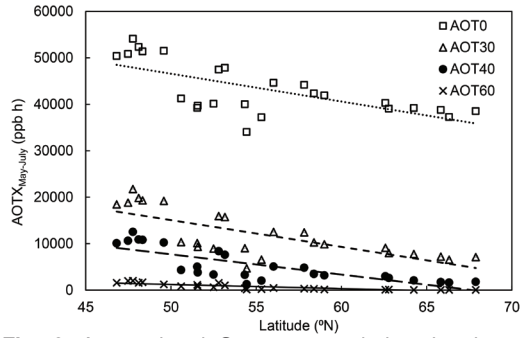

Fig. 6. Accumulated O_3 exposure during the three-month period from May–July over different thresholds: no threshold (AOT0); 30 ppb (AOT30); 40 ppb (AOT40); and 60 ppb (AOT60), as an average from the years 1990–2015, in relation to the latitude of the monitoring station. AOT0: $y = -599.0x + 76500$, $R^2 = 0.46$, $p < 0.001$. AOT30: $y = -576.7x + 43900$, $R^2 = 0.54$, $p < 0.001$. AOT40: $y = -436.2x + 29500$, $R^2 = 0.61$, $p < 0.001$. AOT60: $y = -89.4x + 5680$, $R^2 = 0.73$, $p < 0.001$.

was minimal when data was averaged over the 26-year period (Appendix Fig. A1).

In summary, the latitude explained a large part of the variation in yearly maximum of daytime mean, yearly maximum 90th percentile and the yearly maximum of the 8-hour mean between the stations ($R^2 > 0.69$) as well as for yearly minimum of daytime mean ($R^2 = 0.63$). The $[O_3]$ maxima were higher in the south of the study area while the $[O_3]$ minima were higher in the north. The correlation with latitude was especially strong with the timing of the maximum $[O_3]$ ($R^2 > 0.87$), independent of whether it was expressed as maximum of the daytime mean, maximum of the 90th percentile or the maximum of the 8-hour mean. The annual $[O_3]$ maximum occurred 2–3 months earlier during the year in the north of the study area compared to the southern areas.

Accumulated O_3 exposure

To assess the O_3 impact on vegetation, the relation between latitude and accumulated O_3 exposure during the three-month period from May to July over different thresholds was studied (Fig. 6). No threshold (AOT0), 30 ppb (AOT30), 40 ppb (AOT40) and 60 ppb (AOT60) were

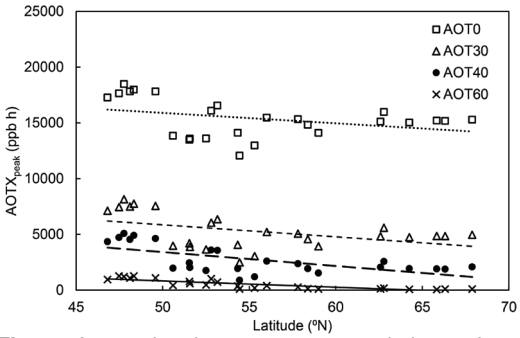

Fig. 7. Accumulated ozone exposure during a four-week period centered around the day of year of maximum daytime mean ozone concentration, in relation to the latitude of the monitoring station. Different thresholds have been used: no threshold (AOT0); 30 ppb (AOT30); 40 ppb (AOT40) and 60 ppb (AOT60). AOTX_{peak} is an average from the years 1990–2015; however, number of years varies between 19–26 since only the years with less than 10% data missing during the accumulation period has been used. AOT0: $y = -93.3x + 20600$, $R^2 = 0.12$, no significance. AOT30: $y = -107.6x + 11200$, $R^2 = 0.20$, $p = 0.027$. AOT40: $y = -124.9x + 9650$, $R^2 = 0.40$, $p < 0.001$. AOT60: $y = -56.5x + 3650$, $R^2 = 0.71$, $p < 0.001$.

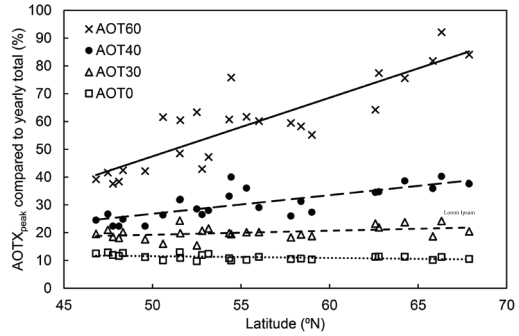

Fig. 8. Accumulated ozone exposure during a four-week period centered around the day of year of maximum daytime mean ozone concentration (AOTX_{peak}) as a percentage of AOTX calculated over the entire year, in relation to the latitude of the monitoring station. It is an average from the years 1990–2015; however number of years varies between 19–26 since only years with less than 10% data missing during the accumulation period has been used. AOT0: $y = -0.1x + 14.8$, $R^2 = 0.19$, $p = 0.029$. AOT30: $y = 0.1x + 12.1$, $R^2 = 0.17$, $p = 0.043$. AOT40: $y = 0.7x - 6.7$, $R^2 = 0.59$, $p < 0.001$. AOT60: $y = 2.1x - 58.0$, $R^2 = 0.76$, $p < 0.001$.

included. For all thresholds, the AOT$X_{May–July}$ was lower in the north. The correlation of the AOTX index with latitude was stronger with higher thresholds.

To assess the O_3 exposure during the time period of annual [O_3] peak, AOTX was calculated during a four-week period centered around the day of year of the maximum daytime mean [O_3] (AOTX_{peak}; Fig. 7). Again, different thresholds were used, no threshold (AOT0), 30 ppb (AOT30), 40 ppb (AOT40) and 60 ppb (AOT60). The AOTX_{peak} showed a tendency for lower values at higher latitudes, statistically significant for AOT40$_{peak}$ and AOT60$_{peak}$. The AOTX_{peak} as a percentage of the AOTX accumulated over the entire year was also calculated (Fig. 8). For AOT40 and AOT60, the AOT accumulated during the [O_3] peak consisted of a large fraction of the yearly exposure, especially in the north.

Temporal trends

Temporal trends over the period from 1990–2015 were investigated using Mann-Kendall analysis. In Table 2, the change per year in the yearly maximum daytime mean (08:00-20:00 local time), the yearly maximum 8-hour mean, the yearly minimum daytime mean [O_3], the day of year of maximum daytime mean [O_3], the AOT40$_{May–July}$ and the AOT$_{peak}$ in percentage of the yearly total exposure is shown.

The yearly maximum daytime mean and the yearly maximum 8-hour mean [O_3] were decreasing at all 25 sites, with statistical significance at 12 and 9 sites, respectively. Also, AOT40 had a declining trend at 24 sites and statistical significance at 13 sites. Except for three sites in the UK where the maximum [O_3] had a significant trend towards an earlier [O_3] maximum, there was no statistically significant trend in the timing of maximum [O_3]. Based on the analysis of the day of year of maximum [O_3], no changes in the timing of the O_3 peak concentrations was found. There was no statistically significant trend in how much of the yearly exposure that occurred during the four weeks centered around the maximum [O_3] (AOTX_{peak}). The yearly minimum daytime mean [O_3] is increasing at 23 out of the 25 sites, with statistical significance at 12 sites.

Table 2. Change per year in the yearly maximum daytime mean (08:00–20:00 local time), yearly maximum 8-hour mean, yearly minimum daytime mean O_3 concentration, the day of year of annual maximum daytime mean ozone concentration, the $AOT40_{May–July}$ and $AOT40_{peak}$ in percentage of the yearly total exposure over the period from 1990–2015 based on Mann-Kendall analysis. Positive trends in red and negative in black, bold values indicate statistically significant ($p < 0.05$). *N* is the number of years and varies, since only years with less than 10% data missing during the relevant period has been used.

ID	Max daytime mean (µg m^{-3} $year^{-1}$)	Max 8-hour mean (µg m^{-3} $year^{-1}$)	Min daytime mean (µg m^{-3} $year^{-1}$)	*N*	Day of year (days $year^{-1}$)	*N*	$AOT40_{May–July}$ (ppb hours $year^{-1}$)	*N*	$AOT40_{peak}$ (% $year^{-1}$)	*N*
SE13	–0.60	–0.33	0.21	24	–1.04	24	–50.0	24	0.08	23
FI22	**–0.93**	–0.88	0.27	24	–0.84	24	**–70.5**	23	–0.34	23
NO15	–0.16	–0.06	0.19	25	–0.05	25	4.6	25	–0.61	25
SE35	–0.28	–0.25	–0.09	25	–0.45	25	–31.6	26	–0.65	25
NO39	**–1.02**	**–1.03**	–0.15	25	–0.65	25	**–70.2**	25	–0.25	23
FI37	**–0.86**	–0.88	0.36	23	–1.20	23	**–125.2**	24	–0.00	23
NO43	–0.25	–0.57	**0.52**	24	0.15	24	–29.9	25	0.23	24
NO01	**–1.34**	**–1.50**	**0.50**	20	–0.33	20	–104.9	21	–0.05	19
SE32	**–0.86**	–0.73	**0.46**	26	–1.25	26	–109.1	25	–0.06	26
SE11	**–1.23**	**–1.18**	**0.21**	26	0.54	26	**–142.4**	25	–0.28	25
GB02	**–1.33**	**–1.84**	**0.31**	26	**–2.43**	26	**–68.2**	25	–0.16	26
GB06	–0.46	–0.91	**0.43**	21	**–2.82**	21	**–36.0**	24	0.39	20
GB14	**–1.20**	**–1.76**	**0.32**	21	**–3.03**	21	**–124.0**	22	0.27	20
DE07	–0.99	–1.07	0.05	23	0.00	23	–131.4	23	–0.69	22
DE02	–1.23	–1.42	0.06	25	–1.37	25	–131.4	24	–0.03	25
GB31	**–1.77**	**–2.20**	0.26	23	–1.28	23	**–179.1**	25	–0.03	22
GB36	**–2.03**	**–2.39**	**0.13**	23	–1.64	23	**–158.6**	24	–0.34	21
NL10	**–1.77**	**–1.67**	0.00	26	–0.57	24	**–163.0**	24	–0.15	24
GB13	**–3.18**	**–3.52**	**0.57**	21	–1.70	21	**–167.6**	23	0.48	20
CZ03	–0.95	–1.06	0.08	21	–0.26	21	**–227.2**	23	–0.20	16
AT46	–0.75	–0.89	**0.11**	25	0.39	25	–38.7	25	–0.19	24
AT43	–0.71	–0.86	0.11	24	–0.64	24	–78.7	25	0.12	23
AT02	–0.79	–0.99	0.12	26	–0.36	26	–116.3	26	–0.11	24
CH03	–0.42	–0.36	**0.09**	25	0.13	25	–54.6	26	–0.15	25
CH02	–0.43	–0.65	**0.09**	25	–0.50	25	–61.9	25	0.23	25

Discussion

Our results, based on 26 years of observations of hourly [O_3] from 25 rural European sites from 1990–2015, clearly indicate a strong latitude dependence in the seasonal [O_3] cycle as well as in a number of important O_3 metrics, including those used to assess the risk for O_3 effects on human health and vegetation. Our investigation shows a distinct pattern in the latitude dependence of the timing of the annual [O_3] peak and its contribution to the annual exposure.

Annual maximum and minimum [O_3]

Ground-level O_3 is closely linked to meteorology and different climate conditions throughout Europe result in large regional differences in [O_3]. The north to south gradient in maximum [O_3] found in this study (with increasing maximum concentrations towards the south) is in agreement with earlier studies, such as Scheel *et al*. (1997) and Torseth *et al*. (2012). It reflects the increase in emissions and availability of O_3 precursors towards the south, in combination with low amounts of UV radiation, limiting photochemical activity at the northerly locations. According to Jonson *et al*. (2006), the [O_3] levels in winter are low in Europe mainly as a result of O_3 titration by NO ($NO + O_3 \rightarrow NO_2 + O_2$) and the low photochemical activity in most areas. Less titration in the north due to less NO availability could be part of the explanation of the spatial pattern in minimum daytime [O_3] as well as seasonal variations in the O_3 contribution from non-European sources.

Several studies have shown a decreasing trend in maximum [O_3] and an increasing trend in minimum [O_3] (Solberg *et al*. 2005, Jonson *et al*. 2006, Andersson *et al*. 2017, Karlsson *et al*. 2017), which is confirmed to occur over a range of latitudes in this study for the time period from 1990–2015. For example, Karlsson *et al*. (2017) analysed changes in percentiles based on hourly [O_3] for eight EMEP monitoring sites in Fennoscandia and ten sites in north-central Europe for six-month summer and winter periods and separated between day and night from 1990–2014. The highest [O_3] during the summer daytime was found to decrease, while most of the summer night-time percentiles were increasing slightly in north-central Europe, but not in Fennoscandia. During wintertime, almost all percentiles have been increasing in north-central Europe during both day- and night-time. The pattern was similar for Fennoscandia.

In a modelling study on Europe, Jonson *et al*. (2006) attribute partially the increase in wintertime [O_3], the decrease in summer [O_3] in large parts of Europe and the decrease in the magnitude of the high [O_3] episodes to the decrease in O_3 precursor emissions. Andersson *et al*. (2017) used a regional chemistry-transport model to quantify the causes of the observed decrease in high [O_3] and increase in low [O_3] of Sweden. They found that rising lower [O_3] were caused by a combination of change in hemispheric background concentrations, meteorology and anthropogenic emissions, whilst the decrease in the highest [O_3] is mainly caused by reductions in European O_3 precursor emissions.

Based on model results from the task force on Hemispheric Transport of Air pollution (HTAP), Jonson *et al*. (2018) found that while O_3 from European sources peaks in the summer months, the contribution from sources outside Europe are largest in the spring months. In spring, the O_3 production over the polluted continents starts to increase while at the same time the lifetime of O_3 in the free troposphere is relatively long. However, the magnitude and origin of the global/hemispheric [O_3] trends are not completely understood. In addition to changes in the contribution from other continents and from wildfires, the exchange across the tropopause and also the circulation within the troposphere itself could have been altered by changing circulation patterns (Jonson *et al*. 2006).

The spring [O_3] maximum at high latitudes

In addition to the changes in the frequency distribution of [O_3] over Europe, a shift of the [O_3] seasonal cycle at northern mid-latitudes has been reported, suggesting that the observed peak

[O_3] now appear earlier in the year compared to previous decades (Parrish *et al*. 2013). Derwent *et al*. (2015) concluded that it is possible that this shift in seasonal cycles at the northern hemisphere mid-latitude baseline O_3 monitoring stations is caused by changing intercontinental O_3 production and transport. In our study, using data from 25 non-marine, non-mountainous stations in central and northern Europe, we could not find evidence for significant changes in the timing of the seasonal cycle based on analysis of the day of year of maximum [O_3]. However, the day of year of maximum [O_3] had a large year-to-year variation, which obstructs the possibility to distinguish trends. The issue of changes in the timing of the yearly [O_3] maximum needs further investigation.

Our results show a latitudinal pattern in the timing of the annual [O_3] maximum, where maximum [O_3] occur earlier in the north. Tanimoto *et al*. (2005) also found that the phase and amplitude of the seasonal cycle in the East Asian Pacific rim region largely depends on latitude. They concluded that the spring [O_3] maximum is modified by changes in the long-range transport, coupled with regional photochemistry.

Several factors have been proposed to contribute to the pronounced and early spring maximum of [O_3] at high latitudes. Transport of O_3 from the stratosphere was suggested to contribute to the seasonal variation in [O_3] e.g., in northern Finland (Hatakka *et al*. 2003) and over the high-altitude western USA (Lin *et al*. 2012). In a review of the observations and origins of the O_3 spring maximum, Monks (2000) concluded that most evidence suggest that there is not a strong seasonal variation in the stratosphere–troposphere O_3 exchange on average. In a study from northeast Asia, Kim and Lee (2010) did not find any evidence supporting that the springtime enhancement was a result of stratospheric intrusion.

The latitudinal variation in the shape of the O_3 seasonal cycle has sometimes been interpreted as a consequence of the apparent north to south gradient in O_3 precursor emissions (Monks 2000). The polar sunrise and fast increase in available radiation stimulates photochemical activity on the arctic winter reservoir of O_3 precursors (Laurila and Hakola 1996). The increased solar radiation in spring also enhances vertical mixing of the air, which supports higher ground-level [O_3] compared to the more stable air stratification typical of the polar winter (Rummukainen *et al*. 1996).

Snow cover can also influence the [O_3] near the ground. The deposition velocity to snow is very low (Galbally and Roy 1980). The deposition velocity increases rapidly as the snow disappears and the vegetation develops a large physiologically active leaf area (Rummukainen *et al*. 1996). In addition, snow has a high albedo, both for visible light and UVA radiation, promoting photolysis of NO_2 and thus O_3 formation (Simpson *et al*. 2002, Schnell *et al*. 2009). To what extent local photochemistry in contrast to long-range transported pollution is responsible for the spring [O_3] maximum needs further investigation.

O_3 risks for health and vegetation

The number of days per year when the maximum 8-hour mean of [O_3] exceeds 120 μg m^{-3} is alarmingly high in the southern part of the study area. According to Karlsson *et al*. (2017) the future yearly maximum 8-hour mean of [O_3] is projected not to exceed the EU EQS target value in northern UK and Fennoscandia after 2020. However, the WHO EQS target value of 100 μg m^{-3} will be exceeded in this region also in the future. As a result, acute impacts on human health can be expected to decrease in the future, but chronic impacts on humans, caused by an 8-hour mean of [O_3] exceeding 70 μg m^{-3} may remain despite the increase. The threshold of 70 μg m^{-3} (35 ppb) is related to the metric SOMO35 used by WHO for the protection of human health.

Within the study area, only the stations south of 50° latitude exceed the $AOT40_{May–July}$ target value of 9000 ppb hours, averaged over all years included in the study. In the far north, the long-term objective of 3000 ppb hours is met. However, the long daylight hours as well as the humid conditions in both air and soil promote O_3 uptake in northern Europe. This means that the phytotoxic impacts of O_3 on vegetation

can be almost as important in northern Europe as they are further south (Simpson *et al*. 2007, Karlsson *et al*. 2009). In combination with an earlier onset of the growing season in mid- and high latitudes, likely associated with global warming (Linderholm 2006, Menzel *et al*. 2006, Karlsson *et al*. 2007), there is a substantial risk for negative O_3 impacts on vegetation in the north of the study area due to an increasing overlap of the growing season and the spring [O_3] maximum at high latitudes.

Conclusions

The most important conclusions from this study were:

- Yearly [O_3] maximum is lower in the northern part of the study area (defined as Europe north of the Alps, from 46°N to 68°N) than in the south.
- Yearly minimum of daytime mean [O_3] is higher in the north of the study area than in the south.
- There is a strong correlation between the day of year when maximum [O_3] occurred and the latitude. The annual maximum in [O_3] occurred earlier in the north than in the south.
- May–July AOT is lower in the north than in the south. AOT40 and AOT60 calculated over four weeks centered at the yearly [O_3] maximum constitute a large part of the yearly exposure, especially in the north of the study area. Thus, the spring/summer maximum in [O_3] represents a larger fraction of the annual O_3 exposure at higher latitudes.
- Maximum daytime mean [O_3], maximum 8-hour mean [O_3] and May–July AOT40 showed a decreasing trend during the time period from (1990–2015) while the minimum daytime mean [O_3] showed an increasing trend.
- No statistically significant trend in the timing of when the maximum [O_3] occurred was found in this study.

Acknowledgements: This research was performed within the SCAC2 and CLEO research programmes funded by the Swedish Environmental Protection Agency.

References

Andersson C., Alpfjord H., Robertson L., Karlsson P.E. & Engardt M. 2017. Reanalysis of and attribution to near-surface ozone concentrations in Sweden during 1990–2013. *Atmospheric Chemistry and Physics* 17: 13869–13890.

Derwent R.G., Utembe S.R., Jenkin M.E. & Shallcross D.E. 2015. Tropospheric ozone production regions and the intercontinental origins of surface ozone over Europe. *Atmospheric Environment* 112: 216–224.

Derwent R.G., Manning A.J., Simmonds P.G., Spain T.G. & O'Doherty S. 2018. Long-term trends in ozone in baseline and European regionally-polluted air at Mace Head, Ireland over a 30-year period. *Atmospheric Environment* 179: 279–287.

EU. 2008. EU Directive 2008/50/EC of the European Parliament and of the Council on Ambient Air Quality and Cleaner Air for Europe 21 May 2008.

Fuhrer J., Skärby L. & Ashmore M.R. 1997. Critical levels for ozone effects on vegetation in Europe. *Environmental Pollution* 97: 91–106.

Galbally I.E. & Roy C.R. 1980. Destruction of ozone at the earth's surface. *Quarterly Journal of the Royal Meteorological Society* 106: 599–620.

Hatakka J., Aalto T., Aaltonen V., Aurela M., Hakola H., Komppula M., Laurila T., Lihavainen H., Paatero J., Salminen K. & Viisanen Y. 2003. Overview of the atmospheric research activities and results at Pallas GAW station. *Boreal Environment Research* 8: 365–383.

IPCC. 2013. Stocker T.F., Qin D., Plattner G.K., Alexander L.V., Allen S.K., Bindoff N.L., Bréon F.-M., Church J.A., Cubasch U., Emori S., Forster P., Friedlingstein P., Gillett N., Gregory J.M., Hartmann D.L., Jansen E., Kirtman B., Knutti R., Krishna Kumar K., Lemke P., Marotzke J., Masson-Delmotte V., Meehl G.A., Mokhov I.I., Piao S., Ramaswamy V., Randall D., Rhein M., Rojas M., Sabine C., Shindell D., Talley L.D., Vaughan D.G. and Xie S.P. Technical Summary. In: Climate Change 2013: The Physical Science Basis. *Contribution of Working Group I to the Fifth Assessment Report of the Intergovernmental Panel on Climate Change*. Edited by Stocker, T.F., Qin D., Plattner G.-K., Tignor M., Allen S.K., Boschung J., Nauels A., Xia Y., Bex V. and Midgley P.M. Cambridge University Press, Cambridge, United Kingdom and New York, NY, USA.

Jonson J.E., Simpson D., Fagerli H. & Solberg S. 2006. Can we explain the trends in European ozone levels? *Atmospheric Chemistry and Physics* 6: 51–66.

Jonson J.E., Schulz M., Emmons L., Flemming J., Henze D., Sudo K., Lund M.T., Lin M., Benedictow A., Koffi B., Dentener F., Keating T., Kivi R. & Davila Y. 2018. The effects of intercontinental emission sources on European air pollution levels. *Atmospheric Chemistry and Physics* 18: 13655–13672.

Karlsen S.R., Tolvanen A., Kubin E., Poikolainen J., Hogda

K.A., Johansen B., Danks F.S., Aspholm P., Wielgolaski F.E. & Makarova O. 2008. MODIS-NDVI-based mapping of the length of the growing season in northern Fennoscandia. *International Journal of Applied Earth Observation and Geoinformation* 10: 253–266.

Karlsson P.E., Pleijel H. & Simpson D. 2009. Ozone Exposure and Impacts on Vegetation in the Nordic and Baltic Countries. *Ambio* 38: 402–405.

Karlsson P.E., Tang L., Sundberg J., Chen D., Lindskog A. & Pleijel H. 2007. Increasing risk for negative ozone impacts on vegetation in northern Sweden. *Environmental Pollution* 150: 96–106.

Karlsson P.E., Klingberg J., Engardt M., Andersson C., Langner J., Karlsson G.P. & Pleijel H. 2017. Past, present and future concentrations of ground-level ozone and potential impacts on ecosystems and human health in northern Europe. *Science of the Total Environment* 576: 22–35.

Kim J.H. & Lee H. 2010. What Causes the Springtime Tropospheric Ozone Maximum over Northeast Asia? *Advances in Atmospheric Sciences* 27: 543–551.

Klingberg J., Björkman M.P., Pihl Karlsson G. & Pleijel H. 2009. Observations of ground-level ozone and NO2 in northernmost Sweden, including the Scandian *Mountain Range Ambio* 38: 448–451.

Klingberg J., Karlsson P.E., Pihl Karlsson G., Hu Y., Chen D. & Pleijel H. 2012. Variation in ozone exposure in the landscape of southern Sweden with consideration of topography and coastal climate. *Atmospheric Environment* 47: 252–260.

Laurila T. & Hakola H. 1996. Seasonal cycle of C2–C5 hydrocarbons over the Baltic Sea and Northern Finland. *Atmospheric Environment* 30: 1597–1607.

Lin M.Y., Fiore A.M., Cooper O.R., Horowitz L.W., Langford A.O., Levy H., Johnson B.J., Naik V., Oltmans S.J. & Senff C.J. 2012. Springtime high surface ozone events over the western United States: Quantifying the role of stratospheric intrusions. *Journal of Geophysical Research: Atmospheres* 117, doi:10.1029/2012JD018151.

Linderholm H.W. 2006. Growing season changes in the last century. *Agricultural and Forest Meteorology* 137: 1–14.

Mann H.B. 1945. Non-parametric tests against trend. *Econometrica* 13: 245–259.

Menzel A., Sparks T.H., Estrella N., Koch E., Aaasa A., Ahas R., Alm-Kübler K., Bissolli P., Braslavska O., Briede A., Chmielewski F.M., Crepinsek Z., Curnel Y., Dahl A., Defila C., Donnelly A., Filella Y., Jatczak K., Måge F., Mestre A., Nordli Ø., Peñuelas J., Pirinen P., Remisova V., Scheifinger H., Striz M., Susnik A., Van Vliet A.J.H., Wielgolaski F.E., Zach S. & Zust A. 2006. European phenological response to climate change matches the warming pattern. *Global Change Biology* 12: 1969–1976.

Monks P.S. 2000. A review of the observations and origins of the spring ozone maximum. *Atmospheric Environment* 34: 3545–3561.

Monks P.S., Archibald A.T., Colette A., Cooper O., Coyle M., Derwent R., Fowler D., Granier C., Law K.S., Mills G.E., Stevenson D.S., Tarasova O., Thouret V., von Schneidemesser E., Sommariva R., Wild O. & Williams M.L. 2015. Tropospheric ozone and its precursors from the urban to the global scale from air quality to short-lived climate forcer. *Atmospheric Chemistry and Physics* 15: 8889–8973.

Narayana Rao T., Arvelius J., Kirkwood S. & von der Gathen P. 2004. Climatology of ozone in the troposphere and lower stratosphere over the European Arctic. *Advances in Space Research* 34: 754–758.

Paoletti E., De Marco A., Beddows D.C.S., Harrison R.M. & Manning W.J. 2014. Ozone levels in European and USA cities are increasing more than at rural sites, while peak values are decreasing. *Environmental Pollution* 192: 295–299.

Parrish D.D., Law K.S., Staehelin J., Derwent R., Cooper O.R., Tanimoto H., Volz-Thomas A., Gilge S., Scheel H.E., Steinbacher M. & Chan E. 2012. Long-term changes in lower tropospheric baseline ozone concentrations at northern mid-latitudes. *Atmospheric Chemistry and Physics* 12: 11485–11504.

Parrish D.D., Law K.S., Staehelin J., Derwent R., Cooper O.R., Tanimoto H., Volz-Thomas A., Gilge S., Scheel H.E., Steinbacher M. & Chan E. 2013. Lower tropospheric ozone at northern midlatitudes: Changing seasonal cycle. *Geophysical Research Letters* 40: 1631–1636.

Pleijel H., Klingberg J., Karlsson G.P., Engardt M. & Karlsson P.E. 2013. Surface ozone in the marine environment - horizontal ozone concentration gradients in coastal areas. *Water Air and Soil Pollution* 224: 1603, doi:10.1007/s11270-013-1603-4.

Royal Society. 2008. *Ground-level ozone in the 21st century: future trends, impacts and policy implications.* RS Policy document 15/08, London (available at http://royalsociety.org).

Rummukainen M., Laurila T. & Kivi R. 1996. Yearly cycle of lower tropospheric ozone at the arctic circle. *Atmospheric Environment* 30: 1875–1885.

Scheel H.E., Areskoug H., Geiss H., Gomiscek B., Granby K., Haszpra L., Klasinc L., Kley D., Laurila T., Lindskog A., Roemer M., Schmitt R., Simmonds P., Solberg S. & Toupance G. 1997. On the spatial distribution and seasonal variation of lower-troposphere ozone over Europe. *Journal of Atmospheric Chemistry* 28: 11–28.

Schnell R.C., Oltmans S.J., Neely R.R., Endres M.S., Molenar J.V. & White A.B. 2009. Rapid photochemical production of ozone at high concentrations in a rural site during winter. *Nature Geoscience* 2: 120–122.

Sen P.K. 1968. Estimates of the regression coefficient based on Kendall's tau. *Journal of the American Statistical Association* 63: 1379–1389.

Sicard P., Serra R. & Rossello P. 2016. Spatiotemporal trends in ground-level ozone concentrations and metrics in France over the time period 1999–2012. *Environmental*

Research 149: 122–144.

Simpson D., Ashmore M.R., Emberson L. & Tuovinen J.P. 2007. A comparison of two different approaches for mapping potential ozone damage to vegetation. A model study. *Environmental Pollution* 146: 715–725.

Simpson W.R., King M.D., Beine H.J., Honrath R.E. & Peterson M.C. 2002. Atmospheric photolysis rate coefficients during the Polar Sunrise Experiment ALERT2000. *Atmospheric Environment* 36: 2471–2480.

Solberg S., Bergström R., Langner J., Laurila T. & Lindskog A. 2005. Changes in Nordic surface ozone episodes due to European emission reductions in the 1990s. *Atmospheric Environment* 39: 179–192.

Tanimoto H., Sawa Y., Matsueda H., Uno I., Ohara T., Yamaji K., Kurokawa J. & Yonemura S. 2005. Significant latitudinal gradient in the surface ozone spring maximum over East Asia. *Geophysical Research Letters* 32, doi:10.1029/2005GL023514.

Torseth K., Aas W., Breivik K., Fjaeraa A.M., Fiebig M., Hjellbrekke A.G., Myhre C.L., Solberg S. & Yttri K.E. 2012. Introduction to the European Monitoring and Evaluation Programme (EMEP) and observed atmospheric composition change during 1972–2009. *Atmospheric Chemistry and Physics* 12: 5447–5481.

Tuovinen J.P. 2000. Assessing vegetation exposure to ozone: properties of the AOT40 index and modifications by deposition modelling. *Environmental Pollution* 109: 361–372.

Tuovinen J.P., Simpson D., Emberson L., Ashmore M. & Gerosa G. 2007. Robustness of modelled ozone exposures and doses. *Environmental Pollution* 146: 578–586.

WHO. 2006. *Air Quality Guidelines. Global Update 2005*. ISBN 92 890 2192 6.

Vingarzan R. 2004. A review of surface ozone background levels and trends. *Atmospheric Environment* 38: 3431–3442.

Appendix

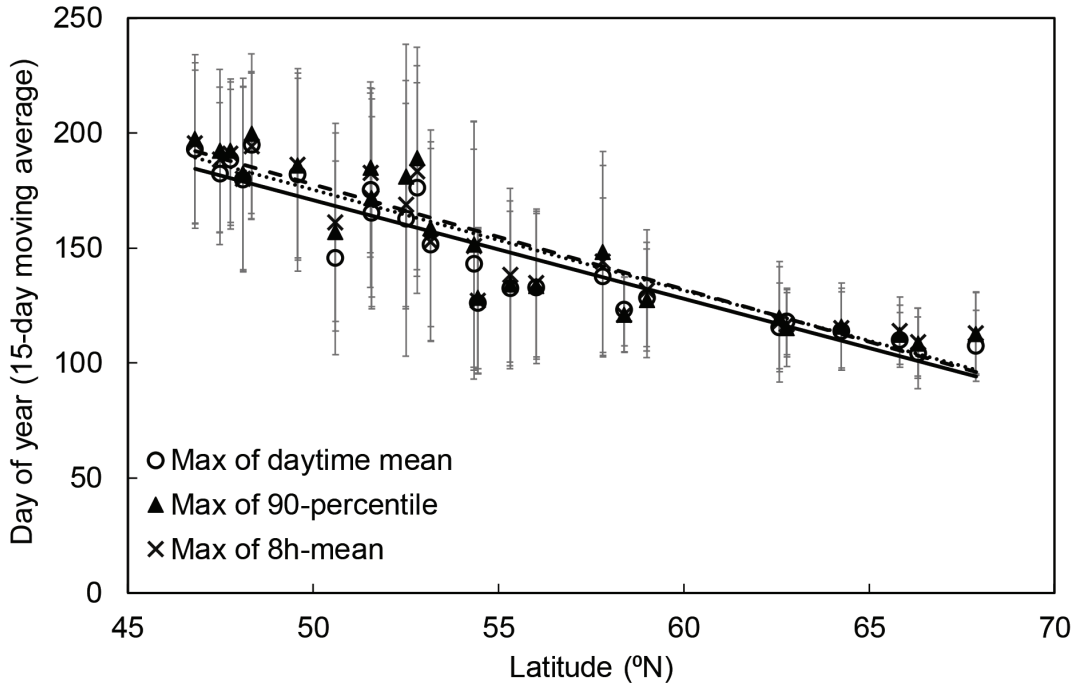

Fig. A1. Day of year when the yearly maximum of daytime mean, the maximum of daily 90th percentile and the maximum of 8-hour mean occurred, as an average from the years 1990–2015, in relation to the latitude of the monitoring station. A 15-day moving average has been applied to the daily data prior to seeking the day of highest [O_3]. Error bars show ±1 SD. Maximum of daytime mean: $y = -4.3x + 385.2$, $R^2 = 0.86$, $p < 0.001$. Maximum of 90th percentile: $y = -4.6x + 405.9$, $R^2 = 0.84$, $p < 0.001$. Maximum of 8-hour mean: $y = -4.4x + 394.2$, $R^2 = 0.86$, $p < 0.001$.